An optimizing implicit difference scheme based on proper orthogonal decomposition for the two-dimensional unsaturated soil water flow equation

Zhenhua Di[1], Zhendong Luo[2,*,†], Zhenghui Xie[3], Aiwen Wang[4] and I. M. Navon[5]

[1]*School of Science, Beijing Jiaotong University, Beijing 100044, China*
[2]*School of Mathematics and Physics, North China Electric Power University, Beijing 102206, China*
[3]*LASG, Institute of Atmospheric Physics, Chinese Academy of Sciences, Beijing 100029, China*
[4]*School of Science, Beijing Information Science and Technology University, Beijing 100192, China*
[5]*Department of Scientific Computing, Florida State University, Dirac Sci. Lib. Bldg., #483, Tallahassee, FL 32306-4120, USA*

SUMMARY

An optimizing reduced implicit difference scheme (IDS) based on singular value decomposition (SVD) and proper orthogonal decomposition (POD) for the two-dimensional unsaturated soil water flow equation is presented. An ensemble of snapshots is compiled from the transient solutions derived from the usual IDS for a two-dimensional unsaturated flow equation. Then, optimal orthogonal bases are reconstructed by implementing SVD and POD techniques for the ensemble of snapshots. Combining POD with a Galerkin projection approach, a new lower dimensional and highly accurate IDS for the two-dimensional unsaturated flow equation is obtained. Error estimates between the true solution, the usual IDS solution, and the reduced IDS solution based on POD basis are derived. Finally, it is shown by means of a numerical example using the technology of local refined grids that the computational load is greatly diminished by using the reduced IDS. Also, the error between the POD approximate solution and the usual IDS solution is proved to be consistent with the derived theoretical results. Thus, both feasibility and efficiency of the POD method are validated. Copyright © 2011 John Wiley & Sons, Ltd.

1. INTRODUCTION

Unsaturated soil water flow is the flow in the portion of the Earth between the land surface and the phreatic zone or zone of saturation, which is an important form of flow in porous media. The unsaturated flow problem is described by a nonlinear partial differential equation (PDE) based on Darcy's law, and numerical discretization methods are the most effective tools to solve this nonlinear PDE. Several studies of soil water flow problem have been presented. For example, Xie *et al.* [1] developed an unsaturated soil water flow numerical model based on a mass-lumped finite element method. Luo *et al.* [2] presented another numerical model to compute soil moisture and water flow

---

flux together by means of a mixed finite element method. In these studies, one-dimensional unsaturated flow equation was employed; thus, there are fewer degrees of freedom, and the computational load is low. Lei *et al.* [3] applied an alternating direction implicit difference scheme (IDS) to solve the two-dimensional unsaturated flow equation for soil moisture content. However, the IDS for the two-dimensional unsaturated flow equation involves a large number of degrees of freedom. So, an important related problem is how to alleviate the computational load and reduce the time required for calculations and memory resource demands in the actual computational process in a way that guarantees sufficient accuracy in the numerical solution.

Proper orthogonal decomposition (POD) is an effective method for approximating a large amount of data. The method essentially finds a group of orthogonal bases from the given data to approximately represent them in a least squares optimal sense. In addition, as the POD is optimal in the least squares sense, it has the property that the model decomposition is completely dependent on the given data and does not require assuming any prior knowledge of the process. Combined with a Galerkin projection procedure, POD provides a powerful method for deriving lower dimensional models of dynamical systems from a high or even infinite dimensional phase space. A dynamic system is generally governed by related structures or the ensemble formed by a large number of different instantaneous solutions, and the POD method can capture the temporal and spatial structures of dynamic system by applying a statistical analysis to the ensemble of data. POD provides an adequate approximation for a large amount of data with a reduced number of degrees of freedom; it alleviates the computational load and provides substantial savings in memory requirements. POD has found widespread application in a variety of fields such as signal analysis and pattern recognition [4, 5], fluid dynamics and coherent structures [6–8], and optimal flow control problems [9, 10]. In fluid dynamics, Lumley first applied the POD method to capture the large eddy coherent structures in a turbulent boundary layer [11]. This method was further applied to study the relation between the turbulent structure and a chaotic dynamic system [12]. Sirovich introduced the method of snapshots and applied it to reduce the order of POD eigenvalue problem [13]. Kunisch and Volkwein presented Galerkin POD methods for parabolic problems and a general equation in fluid dynamics [14, 15]. More recently, a finite difference scheme (FDS) and a mixed finite element (MFE) formulation for the non-stationary Navier–Stokes equation based on POD were derived [16, 17], respectively. Finite element formulation based on POD was also applied for parabolic equations and the Burgers equation [18, 19]. In other physical applications, an effective use of POD for a chemical vapor deposition reactor was demonstrated, and some reduced order FDS and MFE for the upper tropical Pacific Ocean model based on POD were presented [20–24]. An optimizing reduced FDS based on POD for the chemical vapor deposit (CVD) equations was also presented in [25]. Except for POD, the empirical orthogonal function (EOF) analysis is another effective method to extract information from large datasets in time and space [26, 27]. However, to the best of our knowledge, there are no published results addressing the POD approximated solution of IDS (i.e., reduced IDS solution) for the two-dimensional unsaturated soil flow equation and the error estimates between the true solution, the usual IDS solution, and the reduced IDS solution based on POD basis.

In this paper, POD is used to reduce the IDS for the two-dimensional unsaturated soil water flow equation, and the error estimates between the true solution, the usual IDS solution, and the reduced IDS solution are derived. The paper is organized as follows: Section 2 is devoted to describing the IDS for the two-dimensional unsaturated flow equation and generating snapshots from the IDS solutions. The optimizing reduced IDS based on POD technique for the two-dimensional unsaturated flow equation is derived in Section 3. Error estimates between the true solution, the usual IDS solution, and the reduced IDS solution are derived in Section 4. In Section 5, some numerical examples using the technology of local refined grids are presented to validate the theoretical results. Finally, conclusions are provided in Section 6.

2. IMPLICIT DIFFERENCE SCHEME FOR THE TWO-DIMENSIONAL UNSATURATED FLOW EQUATION AND SNAPSHOTS GENERATION

2.1. The two-dimensional unsaturated soil water flow

With an underground pipeline being infiltrated, the soil water moves around the underground pipeline, and the problem is reduced to a two-dimensional unsaturated soil water flow problem

of soil vertical profiles (see Figure 1). A homogeneous and isotropic porous soil medium is considered. As shown in Figure 1, the x-axis and the z-axis denote the horizontal (i.e., positive rightward) and vertical directions (i.e., positive downward), respectively.

According to Darcy's law, the two-dimensional unsaturated soil water flow problem can be expressed as follows (see [28]).

$$\frac{\partial \theta}{\partial t} = \frac{\partial}{\partial x}\left[D(\theta)\frac{\partial \theta}{\partial x}\right] + \frac{\partial}{\partial z}\left[D(\theta)\frac{\partial \theta}{\partial z}\right] - \frac{\partial \tilde{K}(\theta)}{\partial z} + S_{\mathrm{r}}, \quad (x, z, t) \in (0, M) \times (0, \tilde{M}) \times (0, T) \quad (1)$$

where M, $\tilde{M}$, and T are three positive real numbers, $\theta(x, z, t)$ is the volumetric soil moisture content, S_{r} is the source absorption rate, and $\tilde{K}(\theta)$ and $D(\theta)$ are the hydraulic conductivity and the hydraulic diffusivity, respectively. $\tilde{K}(\theta)$ and $D(\theta)$ are formulated as in [29]

$$\begin{cases} \tilde{K}(\theta) = K_{\mathrm{s}}\left(\dfrac{\theta}{\theta_{\mathrm{s}}}\right)^{2b+3} \\ D(\theta) = -\dfrac{bK_{\mathrm{s}}\Psi_{\mathrm{s}}}{\theta_{\mathrm{s}}}\left(\dfrac{\theta}{\theta_{\mathrm{s}}}\right)^{b+2} \end{cases} \quad (2)$$

where θ_{s} is saturated soil moisture content, K_{s} is the saturated hydraulic conductivity, Ψ_{s} is the saturated water potential, and b is a parameter related to the soil property.

The corresponding initial and boundary conditions are expressed as follows.

$$\theta(x, z, 0) = \begin{cases} \dfrac{\theta_0 - \theta_{\mathrm{s}}}{M_1}x + \dfrac{\theta_0 - \theta_{\mathrm{s}}}{\tilde{M}_1}z + \theta_{\mathrm{s}}, & x \in (0, M_1], z \in (0, \tilde{M}_1], \dfrac{x}{M_1} + \dfrac{z}{\tilde{M}_1} \leqslant 1 \\ \theta_0, & x \in [M_1, M], z \in [\tilde{M}_1, \tilde{M}] \end{cases} \quad (3)$$

$$\theta(0, 0, t) = \theta_{\mathrm{s}}, \qquad t \in (0, T] \quad (4)$$

$$-D(\theta)\frac{\partial \theta}{\partial z} + \tilde{K}(\theta) = 0, \qquad z = 0, x \in (0, M], t \in (0, T] \quad (5)$$

$$-D(\theta)\frac{\partial \theta}{\partial x} = 0, \qquad x = 0, z \in (0, \tilde{M}], t \in (0, T] \quad (6)$$

$$-D(\theta)\frac{\partial \theta}{\partial z} + \tilde{K}(\theta) = 0, \qquad z = \tilde{M}, x \in (0, M], t \in (0, T] \quad (7)$$
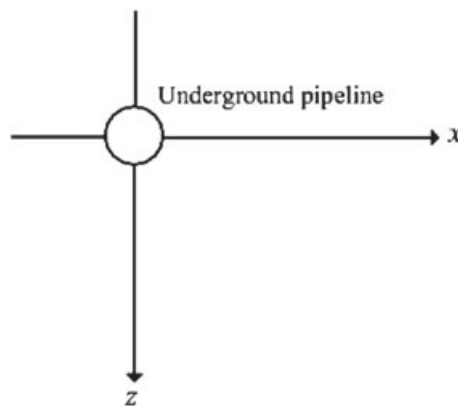
Figure 1. Soil profile for the leakage from underground pipeline.

$$-D(\theta)\frac{\partial\theta}{\partial x}=0, \qquad x=M, z\in(0,\tilde{M}], t\in(0,T] \tag{8}$$

where $\theta_0>0$ is initial soil moisture content, and $z=\tilde{M}$ and $x=M$ represent the lower boundary and the right boundary of the domain, respectively. We suppose that θ_0 and S_r are both smooth enough to ensure the analysis validity.

2.2. The discretization of the two-dimensional unsaturated flow equation and snapshots generation

Obviously, Equation (1) is a nonlinear partial differential equation (PDE), and it is difficult to obtain its analytical solution. However, obtaining an approximated numerical solution by numerical computation method become very popular with the advent of computer technology. So, the numerical computation of Equation (1) is conducted by means of IDS in this paper.

Figure 2 shows the rectangular soil vertical profile with width M and height $\tilde{M}$, which has been discretized into $J\times K$ square cells. Cell nodes are described with a two-dimensional coordinate system (j,k) $(j=0,1,\ldots,J; k=0,1,\ldots,K)$.

In the following, we apply IDS to discretize Equation (1) at each cell node, and assume S_r equal to zero. The five case studies are listed as follows.

(I)   When $k=0$ and Equation (5) are combined, the discretizations of Equation (1) on these nodes are written as follows:

$$\frac{\theta_{j,0}^{n+1}-\theta_{j,0}^{n}}{\Delta t}=D_{j+\frac{1}{2},0}^{n+1}\left(\frac{\theta_{j+1,0}^{n+1}-\theta_{j,0}^{n+1}}{\Delta x^2}\right)-D_{j-\frac{1}{2},0}^{n+1}\left(\frac{\theta_{j,0}^{n+1}-\theta_{j-1,0}^{n+1}}{\Delta x^2}\right)$$
$$+D_{j,\frac{1}{2}}^{n+1}\left(\frac{\theta_{j,1}^{n+1}-\theta_{j,0}^{n+1}}{\Delta z^2}\right)-\frac{1}{\Delta z}\tilde{K}_{j,\frac{1}{2}}^{n+1}, j=1,2,\ldots,J-1 \tag{9}$$

which yields

$$\left(-\frac{\Delta t}{\Delta x^2}D_{j-\frac{1}{2},0}^{n+1}\right)\theta_{j-1,0}^{n+1}+\left(1+\frac{\Delta t}{\Delta x^2}D_{j+\frac{1}{2},0}^{n+1}+\frac{\Delta t}{\Delta x^2}D_{j-\frac{1}{2},0}^{n+1}+\frac{\Delta t}{\Delta z^2}D_{j,\frac{1}{2}}^{n+1}\right)\theta_{j,0}^{n+1}$$
$$+\left(-\frac{\Delta t}{\Delta x^2}D_{j+\frac{1}{2},0}^{n+1}\right)\theta_{j+1,0}^{n+1}+\left(-\frac{\Delta t}{\Delta z^2}D_{j,\frac{1}{2}}^{n+1}\right)\theta_{j,1}^{n+1}=\theta_{j,0}^{n}-\frac{\Delta t}{\Delta z}\tilde{K}_{j,\frac{1}{2}}^{n+1}, j=1,2,\ldots,J-1 \tag{10}$$
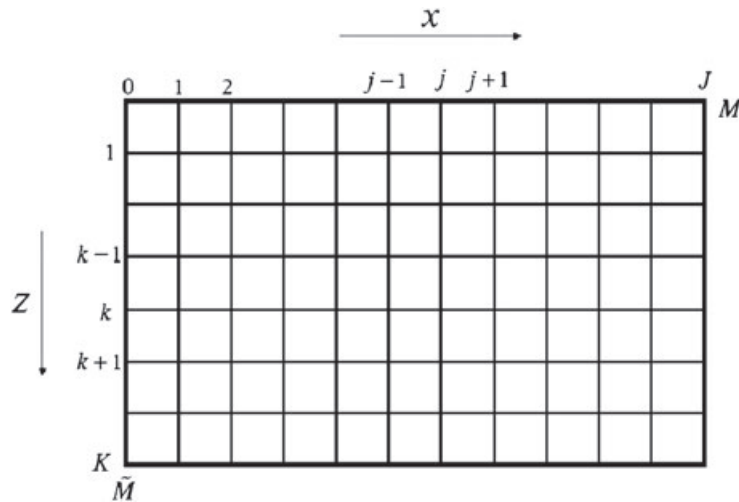
Figure 2. The rectangular soil vertical profile with width M and height $\tilde{M}$ is composed of $J\times K$ square cells.

$$\theta_{j,0}^{n+1} = \theta_{\mathrm{s}}, \ j = 0 \tag{11}$$

$$\frac{\theta_{j,0}^{n+1} - \theta_{j,0}^n}{\Delta t} = -D_{j-\frac{1}{2},0}^{n+1}\left(\frac{\theta_{j,0}^{n+1} - \theta_{j-1,0}^{n+1}}{\Delta x^2}\right) + D_{j,\frac{1}{2}}^{n+1}\left(\frac{\theta_{j,1}^{n+1} - \theta_{j,0}^{n+1}}{\Delta z^2}\right) - \frac{1}{\Delta z}\tilde{K}_{j,\frac{1}{2}}^{n+1}, \ j = J \tag{12}$$

which yields

$$\left(-\frac{\Delta t}{\Delta x^2}D_{j-\frac{1}{2},0}^{n+1}\right)\theta_{j-1,0}^{n+1} + \left(1 + \frac{\Delta t}{\Delta x^2}D_{j-\frac{1}{2},0}^{n+1} + \frac{\Delta t}{\Delta z^2}D_{j,\frac{1}{2}}^{n+1}\right)\theta_{j,0}^{n+1}$$
$$+ \left(-\frac{\Delta t}{\Delta z^2}D_{j,\frac{1}{2}}^{n+1}\right)\theta_{j,1}^{n+1} = \theta_{j,0}^n - \frac{\Delta t}{\Delta z}\tilde{K}_{j,\frac{1}{2}}^{n+1}, \ j = J \tag{13}$$

(II) When $j = 0$ and Equation (6) are combined, the discretizations of Equation (1) on these nodes are written as follows:

$$\frac{\theta_{0,k}^{n+1} - \theta_{0,k}^n}{\Delta t} = D_{\frac{1}{2},k}^{n+1}\left(\frac{\theta_{1,k}^{n+1} - \theta_{0,k}^{n+1}}{\Delta x^2}\right) + D_{0,k+\frac{1}{2}}^{n+1}\left(\frac{\theta_{0,k+1}^{n+1} - \theta_{0,k}^{n+1}}{\Delta z^2}\right) - D_{0,k-\frac{1}{2}}^{n+1}\left(\frac{\theta_{0,k}^{n+1} - \theta_{0,k-1}^{n+1}}{\Delta z^2}\right)$$
$$- \frac{1}{\Delta z}\left(\tilde{K}_{0,k+\frac{1}{2}}^{n+1} - \tilde{K}_{0,k-\frac{1}{2}}^{n+1}\right), \ k = 1, 2, \ldots, K-1 \tag{14}$$

which yields

$$\left(-\frac{\Delta t}{\Delta z^2}D_{0,k-\frac{1}{2}}^{n+1}\right)\theta_{0,k-1}^{n+1} + \left(1 + \frac{\Delta t}{\Delta z^2}D_{0,k+\frac{1}{2}}^{n+1} + \frac{\Delta t}{\Delta z^2}D_{0,k-\frac{1}{2}}^{n+1} + \frac{\Delta t}{\Delta x^2}D_{\frac{1}{2},k}^{n+1}\right)\theta_{0,k}^{n+1}$$
$$+ \left(-\frac{\Delta t}{\Delta x^2}D_{\frac{1}{2},k}^{n+1}\right)\theta_{1,k}^{n+1} + \left(-\frac{\Delta t}{\Delta z^2}D_{0,k+\frac{1}{2}}^{n+1}\right)\theta_{0,k+1}^{n+1} = \theta_{0,k}^n - \frac{\Delta t}{\Delta z}\left(\tilde{K}_{0,k+\frac{1}{2}}^{n+1} - \tilde{K}_{0,k-\frac{1}{2}}^{n+1}\right),$$
$$k = 1, 2, \ldots, K-1 \tag{15}$$

$$\theta_{0,k}^{n+1} = \theta_{\mathrm{s}}, \ k = 0 \tag{16}$$

$$\frac{\theta_{0,k}^{n+1} - \theta_{0,k}^n}{\Delta t} = D_{\frac{1}{2},k}^{n+1}\left(\frac{\theta_{1,k}^{n+1} - \theta_{0,k}^{n+1}}{\Delta x^2}\right) - D_{0,k-\frac{1}{2}}^{n+1}\left(\frac{\theta_{0,k}^{n+1} - \theta_{0,k-1}^{n+1}}{\Delta z^2}\right) + \frac{1}{\Delta z}\tilde{K}_{0,k-\frac{1}{2}}^{n+1}, \ k = K \tag{17}$$

which yields

$$\left(-\frac{\Delta t}{\Delta z^2}D_{0,k-\frac{1}{2}}^{n+1}\right)\theta_{0,k-1}^{n+1} + \left(1 + \frac{\Delta t}{\Delta x^2}D_{\frac{1}{2},k}^{n+1} + \frac{\Delta t}{\Delta z^2}D_{0,k-\frac{1}{2}}^{n+1}\right)\theta_{0,k}^{n+1} + \left(-\frac{\Delta t}{\Delta x^2}D_{\frac{1}{2},k}^{n+1}\right)\theta_{1,k}^{n+1}$$
$$= \theta_{0,k}^n + \frac{\Delta t}{\Delta z}\tilde{K}_{0,k-\frac{1}{2}}^{n+1}, \ k = K \tag{18}$$

(III) When $k = K$ and Equation (7) are combined, the discretizations of Equation (1) on these nodes are written as follows:

$$\frac{\theta_{j,K}^{n+1} - \theta_{j,K}^n}{\Delta t} = D_{j+\frac{1}{2},K}^{n+1}\left(\frac{\theta_{j+1,K}^{n+1} - \theta_{j,K}^{n+1}}{\Delta x^2}\right) - D_{j-\frac{1}{2},K}^{n+1}\left(\frac{\theta_{j,K}^{n+1} - \theta_{j-1,K}^{n+1}}{\Delta x^2}\right)$$
$$- D_{j,K-\frac{1}{2}}^{n+1}\left(\frac{\theta_{j,K}^{n+1} - \theta_{j,K-1}^{n+1}}{\Delta z^2}\right) + \frac{1}{\Delta z}\tilde{K}_{j,K-\frac{1}{2}}^{n+1}, \ j = 1, 2, \ldots, J-1 \tag{19}$$

which yields

$$
\left(-\frac{\Delta t}{\Delta z^2} D^{n+1}_{j,K-\frac{1}{2}}\right)\theta^{n+1}_{j,K-1} + \left(-\frac{\Delta t}{\Delta x^2} D^{n+1}_{j-\frac{1}{2},K}\right)\theta^{n+1}_{j-1,K}
$$

$$
+ \left(1 + \frac{\Delta t}{\Delta x^2} D^{n+1}_{j+\frac{1}{2},K} + \frac{\Delta t}{\Delta x^2} D^{n+1}_{j-\frac{1}{2},K} + \frac{\Delta t}{\Delta z^2} D^{n+1}_{j,K-\frac{1}{2}}\right)\theta^{n+1}_{j,K}
$$

$$
+ \left(-\frac{\Delta t}{\Delta x^2} D^{n+1}_{j+\frac{1}{2},K}\right)\theta^{n+1}_{j+1,K} = \theta^n_{j,K} + \frac{\Delta t}{\Delta z}\tilde{K}^{n+1}_{j,K-\frac{1}{2}}, \ j = 1,2,\ldots,J-1 \qquad (20)
$$

$$
\frac{\theta^{n+1}_{j,K} - \theta^n_{j,K}}{\Delta t} = D^{n+1}_{j+\frac{1}{2},K}\left(\frac{\theta^{n+1}_{j+1,K} - \theta^{n+1}_{j,K}}{\Delta x^2}\right) - D^{n+1}_{j,K-\frac{1}{2}}\left(\frac{\theta^{n+1}_{j,K} - \theta^{n+1}_{j,K-1}}{\Delta z^2}\right) + \frac{1}{\Delta z}\tilde{K}^{n+1}_{j,K-\frac{1}{2}}, \ j = 0
$$

$$(21)$$

which yields

$$
\left(-\frac{\Delta t}{\Delta z^2} D^{n+1}_{j,K-\frac{1}{2}}\right)\theta^{n+1}_{j,K-1} + \left(1 + \frac{\Delta t}{\Delta x^2} D^{n+1}_{j+\frac{1}{2},K} + \frac{\Delta t}{\Delta z^2} D^{n+1}_{j,K-\frac{1}{2}}\right)\theta^{n+1}_{j,K}
$$

$$
+ \left(-\frac{\Delta t}{\Delta x^2} D^{n+1}_{j+\frac{1}{2},K}\right)\theta^{n+1}_{j+1,K} = \theta^n_{j,K} + \frac{\Delta t}{\Delta z}\tilde{K}^{n+1}_{j,K-\frac{1}{2}}, \ j = 0 \qquad (22)
$$

$$
\frac{\theta^{n+1}_{j,K} - \theta^n_{j,K}}{\Delta t} = -D^{n+1}_{j-\frac{1}{2},K}\left(\frac{\theta^{n+1}_{j,K} - \theta^{n+1}_{j-1,K}}{\Delta x^2}\right) - D^{n+1}_{j,K-\frac{1}{2}}\left(\frac{\theta^{n+1}_{j,K} - \theta^{n+1}_{j,K-1}}{\Delta z^2}\right) + \frac{1}{\Delta z}\tilde{K}^{n+1}_{j,K-\frac{1}{2}}, j = J
$$

$$(23)$$

which yields

$$
\left(-\frac{\Delta t}{\Delta z^2} D^{n+1}_{j,K-\frac{1}{2}}\right)\theta^{n+1}_{j,K-1} + \left(-\frac{\Delta t}{\Delta x^2} D^{n+1}_{j-\frac{1}{2},K}\right)\theta^{n+1}_{j-1,K} + \left(1 + \frac{\Delta t}{\Delta x^2} D^{n+1}_{j-\frac{1}{2},K} + \frac{\Delta t}{\Delta z^2} D^{n+1}_{j,K-\frac{1}{2}}\right)\theta^{n+1}_{j,K}
$$

$$
= \theta^n_{j,K} + \frac{\Delta t}{\Delta z}\tilde{K}^{n+1}_{j,K-\frac{1}{2}}, \ j = J \qquad (24)
$$

(IV) When $j = J$ and Equation (8) are combined, the discretizations of Equation (1) on these nodes are written as follows:

$$
\frac{\theta^{n+1}_{J,k} - \theta^n_{J,k}}{\Delta t} = -D^{n+1}_{J-\frac{1}{2},k}\left(\frac{\theta^{n+1}_{J,k} - \theta^{n+1}_{J-1,k}}{\Delta x^2}\right) + D^{n+1}_{J,k+\frac{1}{2}}\left(\frac{\theta^{n+1}_{J,k+1} - \theta^{n+1}_{J,k}}{\Delta z^2}\right)
$$

$$
- D^{n+1}_{J,k-\frac{1}{2}}\left(\frac{\theta^{n+1}_{J,k} - \theta^{n+1}_{J,k-1}}{\Delta z^2}\right) - \frac{1}{\Delta z}\left(\tilde{K}^{n+1}_{J,k+\frac{1}{2}} - \tilde{K}^{n+1}_{J,k-\frac{1}{2}}\right), \ k = 1,2,\ldots,K-1
$$

$$(25)$$

which yields

$$
\left(-\frac{\Delta t}{\Delta z^2} D^{n+1}_{J,k-\frac{1}{2}}\right)\theta^{n+1}_{J,k-1} + \left(1 + \frac{\Delta t}{\Delta z^2} D^{n+1}_{J,k+\frac{1}{2}} + \frac{\Delta t}{\Delta z^2} D^{n+1}_{J,k-\frac{1}{2}} + \frac{\Delta t}{\Delta x^2} D^{n+1}_{J-\frac{1}{2},k}\right)\theta^{n+1}_{J,k}
$$

$$
+ \left(-\frac{\Delta t}{\Delta x^2} D^{n+1}_{J-\frac{1}{2},k}\right)\theta^{n+1}_{J-1,k} + \left(-\frac{\Delta t}{\Delta z^2} D^{n+1}_{J,k+\frac{1}{2}}\right)\theta^{n+1}_{J,k+1}
$$

$$
= \theta^n_{J,k} - \frac{\Delta t}{\Delta z}\left(\tilde{K}^{n+1}_{J,k+\frac{1}{2}} - \tilde{K}^{n+1}_{J,k-\frac{1}{2}}\right), \ k = 1,2,\ldots,K-1 \quad (26)
$$

$$
\frac{\theta^{n+1}_{J,k} - \theta^n_{J,k}}{\Delta t} = -D^{n+1}_{J-\frac{1}{2},k}\left(\frac{\theta^{n+1}_{J,k} - \theta^{n+1}_{J-1,k}}{\Delta x^2}\right) + D^{n+1}_{J,k+\frac{1}{2}}\left(\frac{\theta^{n+1}_{J,k+1} - \theta^{n+1}_{J,k}}{\Delta z^2}\right) - \frac{1}{\Delta z}\tilde{K}^{n+1}_{J,k+\frac{1}{2}}, \ k = 0
$$

$$(27)$$

which yields

$$\left(-\frac{\Delta t}{\Delta x^2}D_{J-\frac{1}{2},k}^{n+1}\right)\theta_{J-1,k}^{n+1}+\left(1+\frac{\Delta t}{\Delta x^2}D_{J-\frac{1}{2},k}^{n+1}+\frac{\Delta t}{\Delta z^2}D_{J,k+\frac{1}{2}}^{n+1}\right)\theta_{J,k}^{n+1}+\left(-\frac{\Delta t}{\Delta z^2}D_{J,k+\frac{1}{2}}^{n+1}\right)\theta_{J,k+1}^{n+1}$$

$$=\theta_{J,k}^n-\frac{\Delta t}{\Delta z}K_{J,k+\frac{1}{2}}^{n+1},\ k=0 \tag{28}$$

$$\frac{\theta_{J,k}^{n+1}-\theta_{J,k}^n}{\Delta t}=-D_{J-\frac{1}{2},k}^{n+1}\left(\frac{\theta_{J,k}^{n+1}-\theta_{J-1,k}^{n+1}}{\Delta x^2}\right)-D_{J,k-\frac{1}{2}}^{n+1}\left(\frac{\theta_{J,k}^{n+1}-\theta_{J,k-1}^{n+1}}{\Delta z^2}\right)+\frac{1}{\Delta z}\tilde{K}_{J,k-\frac{1}{2}}^{n+1},\ k=K \tag{29}$$

which yields

$$\left(-\frac{\Delta t}{\Delta z^2}D_{J,k-\frac{1}{2}}^{n+1}\right)\theta_{J,k-1}^{n+1}+\left(-\frac{\Delta t}{\Delta x^2}D_{J-\frac{1}{2},k}^{n+1}\right)\theta_{J-1,k}^{n+1}+\left(1+\frac{\Delta t}{\Delta x^2}D_{J-\frac{1}{2},k}^{n+1}+\frac{\Delta t}{\Delta z^2}D_{J,k-\frac{1}{2}}^{n+1}\right)\theta_{J,k}^{n+1}$$

$$=\theta_{J,k}^n+\frac{\Delta t}{\Delta z}\tilde{K}_{J,k-\frac{1}{2}}^{n+1},\ k=K \tag{30}$$

(V) For inner cell nodes (j,k) $(j=1,2,\ldots,J-1;\ k=1,2,\ldots,K-1)$, IDS for Equation (1) are expressed as follows:

$$\frac{\theta_{j,k}^{n+1}-\theta_{j,k}^n}{\Delta t}=D_{j+\frac{1}{2},k}^{n+1}\left(\frac{\theta_{j+1,k}^{n+1}-\theta_{j,k}^{n+1}}{\Delta x^2}\right)-D_{j-\frac{1}{2},k}^{n+1}\left(\frac{\theta_{j,k}^{n+1}-\theta_{j-1,k}^{n+1}}{\Delta x^2}\right)$$

$$+D_{j,k+\frac{1}{2}}^{n+1}\left(\frac{\theta_{j,k+1}^{n+1}-\theta_{j,k}^{n+1}}{\Delta z^2}\right)-D_{j,k-\frac{1}{2}}^{n+1}\left(\frac{\theta_{j,k}^{n+1}-\theta_{j,k-1}^{n+1}}{\Delta z^2}\right) \tag{31}$$

$$-\frac{1}{\Delta z}\left(\tilde{K}_{j,k+\frac{1}{2}}^{n+1}-\tilde{K}_{j,k-\frac{1}{2}}^{n+1}\right),\ j=1,2,\ldots,J-1;\ k=1,2,\ldots,K-1$$

which yields

$$\left(-\frac{\Delta t}{\Delta x^2}D_{j-\frac{1}{2},k}^{n+1}\right)\theta_{j-1,k}^{n+1}+\left(-\frac{\Delta t}{\Delta x^2}D_{j+\frac{1}{2},k}^{n+1}\right)\theta_{j+1,k}^{n+1}$$

$$+\left(1+\frac{\Delta t}{\Delta x^2}D_{j+\frac{1}{2},k}^{n+1}+\frac{\Delta t}{\Delta x^2}D_{j-\frac{1}{2},k}^{n+1}+\frac{\Delta t}{\Delta z^2}D_{j,k+\frac{1}{2}}^{n+1}+\frac{\Delta t}{\Delta z^2}D_{j,k-\frac{1}{2}}^{n+1}\right)\theta_{j,k}^{n+1}$$

$$+\left(-\frac{\Delta t}{\Delta z^2}D_{j,k-\frac{1}{2}}^{n+1}\right)\theta_{j,k-1}^{n+1}+\left(-\frac{\Delta t}{\Delta z^2}D_{j,k+\frac{1}{2}}^{n+1}\right)\theta_{j,k+1}^{n+1}$$

$$=\theta_{j,k}^n-\frac{\Delta t}{\Delta z}\left(\tilde{K}_{j,k+\frac{1}{2}}^{n+1}-\tilde{K}_{j,k-\frac{1}{2}}^{n+1}\right),\ j=1,2,\ldots,J-1;\ k=1,2,\ldots,K-1 \tag{32}$$

2.3. Implementation of the numerical algorithm for two-dimensional unsaturated flow equation

The coefficient matrix of IDS (10), (11), (13), (15), (16), (18), (20), (22), (24), (26), (28), (30), and (32) is strictly diagonally dominant, so the IDS has a unique solution. In the following, we give the implementation of algorithm for solving IDS (10), (11), (13), (15), (16), (18), (20), (22), (24), (26), (28), (30), and (32) from nth step to $(n+1)$th step, which consists of five steps.

Step 1. Let $D_{j\pm\frac{1}{2},k}^{n+1}=\left(D_{j,k}^{n+1}D_{j\pm1,k}^{n+1}\right)^{\frac{1}{2}}$, $D_{j,k\pm\frac{1}{2}}^{n+1}=\left(D_{j,k}^{n+1}D_{j,k\pm1}^{n+1}\right)^{\frac{1}{2}}$, $\tilde{K}_{j\pm\frac{1}{2},k}^{n+1}=\left(\tilde{K}_{j,k}^{n+1}\tilde{K}_{j\pm1,k}^{n+1}\right)^{\frac{1}{2}}$,

and $\tilde{K}_{j,k\pm\frac{1}{2}}^{n+1}=\left(\tilde{K}_{j,k}^{n+1}\tilde{K}_{j,k\pm1}^{n+1}\right)^{\frac{1}{2}}$, $(j=0,1,2,\ldots,J;\ k=0,1,2,\ldots,K;\ n=1,2,\ldots,N)$ for the calculation of the IDS equations depending on given $\theta_{j,k}^n$ $(j=0,1,2,\ldots,J;\ k=0,1,2,\ldots,K;\ n=0,1,2,\ldots,N-1)$.

Step 2. Write $\theta_i^n = \theta_{j,k}^n$ $(i = k(J + 1) + (j + 1)$, $m = (J + 1)(K + 1)$, $i = 1, 2, \ldots, m$; $j = 0, 1, 2, \ldots, J$; $k = 0, 1, 2, \ldots, K$; $n = 0, 1, \ldots, N - 1)$. For given θ_i^n $(i = 1, 2, \ldots, m$; $n = 0, 1, 2, \ldots, N - 1)$, compute $D(\theta_i^n)$ and $\tilde{K}(\theta_i^n)$ with Equation (2) and endow with $D_i^n \equiv D(\theta_i^n)$ and $\tilde{K}_i^n \equiv \tilde{K}(\theta_i^n)$ $(i = 1, 2, \ldots, m$; $n = 0, 1, \ldots, N - 1)$. Similarly, the coefficient matrix of IDS (10), (11), (13), (15), (16), (18), (20), (22), (24), (26), (28), (30), and (32) is a matrix depending on Δt, Δx^2, Δz^2, and D_i^{n+1} $\tilde{K}_i^{n+1}$.

Step 3. Solve (10), (11), (13), (15), (16), (18), (20), (22), (24), (26), (28), (30), and (32) by replacing D_i^{n+1} and $\tilde{K}_i^{n+1}$ in their coefficient matrix and right-hand-side term with D_i^n and $\tilde{K}_i^n$ (i.e., $D_i^n \Rightarrow D_i^{n+1}$ and $\tilde{K}_i^n \Rightarrow \tilde{K}_i^{n+1}$) yields θ_i^{n+1} $(i = 1, 2, \ldots, m$; $n = 0, 1, 2, \ldots, N - 1)$ as pre-estimate value.

Step 4. Update D_i^{n+1} and $\tilde{K}_i^{n+1}$ in coefficient matrix and right-hand-side term with pre-estimate value θ_i^{n+1} $(i = 1, 2, \ldots, m$; $n = 0, 1, 2, \ldots, N - 1)$ by Equation (2).

Step 5. Repeat steps 3 and 4 until θ_i^{n+1} $(i = 1, 2, \ldots, m$; $n = 0, 1, 2, \ldots, N - 1)$ are found out.

Thus, we may take $m \times L$ group of values consisting of the ensemble $\{\theta_i^l\}_{l=1}^L$ $(1 \leqslant i \leqslant m)$ (usually $L \ll N$, known as 'snapshots' in POD method) from $m \times N$ group of $\{\theta_i^n\}_{n=1}^N$ $(1 \leqslant i \leqslant m)$.

Remark 1
In real-life problems, the ensemble of snapshots is usually obtained from the previous experiments or simulation results. We then restructure the optimal basis for the ensemble of snapshots by the following POD and finally combine them with the Galerkin projection to produce a reduced dynamical system model. Thus, the variation of soil moisture content can be quickly simulated, which is of great practical value in actual real-life applications.

3. POD REDUCED MODEL FOR THE TWO-DIMENSIONAL UNSATURATED FLOW EQUATION

In this section, we first find the POD basis from the ensemble of snapshots generated in Section 2 and then use the POD basis to construct a reduced optimizing IDS for two-dimensional unsaturated flow equation.

3.1. Singular value decomposition and proper orthogonal decomposition optimal basis

The ensemble of snapshots $\{\theta_i^l\}_{l=1}^L$ $(1 \leqslant i \leqslant m)$ can be written as a $m \times L$ matrix A as follows:

$$A = \begin{pmatrix} \theta_1^1 & \theta_1^2 & \cdots & \theta_1^L \\ \theta_2^1 & \theta_2^2 & \cdots & \theta_2^L \\ \vdots & \vdots & \vdots & \vdots \\ \theta_m^1 & \theta_m^2 & \cdots & \theta_m^L \end{pmatrix} \tag{33}$$

Singular value decomposition (SVD) is an important tool for finding the optimal orthogonal basis of matrix column vectors. For the matrix $A \in R^{m \times L}$, there exists the SVD:

$$A = U \begin{pmatrix} S & 0 \\ 0 & 0 \end{pmatrix} V^T \tag{34}$$

where $U \in R^{m \times m}$ and $V \in R^{L \times L}$ are orthogonal matrices, $S = \text{diag}\{\sigma_1, \sigma_2, \ldots, \sigma_\ell\} \in R^{\ell \times \ell}$ is the diagonal matrix correspondent to A, and $\sigma_i (i = 1, 2, \ldots, \ell)$ are positive singular values. The matrices of $U = (\phi_1, \phi_2, \ldots \phi_m) \in R^{m \times m}$ and $V = (\varphi_1, \varphi_2, \ldots \varphi_L) \in R^{L \times L}$ contain the orthogonal eigenvectors to the AA^T and $A^T A$, respectively. The columns of these eigenvector matrices are arranged so that the corresponding singular values σ_i $(i = 1, 2, \ldots, \ell)$ comprised in S are in a non-increasing order. The singular values of the decomposition and the eigenvalue of the matrices AA^T and $A^T A$ satisfy the relations: $\lambda_i = \sigma_i^2$ $(i = 1, 2, \ldots, \ell)$. The number of grid nodes is far

larger than that of transient moment points (i.e., $m \gg L$), that is, the order m for matrix $A A^T$ is far larger than the order L for matrix $A^T A$. However, their non-null eigenvalues are identical; therefore, we first solve the eigen-equation of matrix $A^T A$ to find the eigenvectors $\boldsymbol{\varphi}_j$ ($j = 1, 2, \ldots, L$), and then the ℓ ($\ell \ll L$) eigenvectors $\boldsymbol{\phi}_j$ ($j = 1, 2, \ldots, \ell$) corresponding to the non-null eigenvalues for matrix $A A^T$ are obtained by the relationship:

$$\boldsymbol{\phi}_j = \frac{1}{\sigma_j} A \boldsymbol{\varphi}_j, \qquad j = 1, 2, \ldots, \ell \tag{35}$$

Define the matrix norm $\| \bullet \|_{\alpha, \beta}$ as $\|A\|_{\alpha, \beta} = \sup_{x \neq 0} \frac{\|A x\|_\alpha}{\|x\|_\beta}$ (where $\| \bullet \|_\alpha$ and $\| \bullet \|_\beta$ are the vector norms). According to the relationship between spectral radius and the matrix norm $\| \bullet \|_{2,2}$, if $M_\theta < r = \text{rank } A$ ($r \leqslant \ell \leqslant L$), there is the following equation:

$$\sigma_{(M_\theta + 1)} = \min_{\text{rank}(\beta) \leqslant M_\theta} \|A - B\|_{2,2} = \|A - A_{M_\theta}\|_{2,2} \tag{36}$$

where $A_{M_\theta} = \sum\limits_{i=1}^{M_\theta} \sigma_i \boldsymbol{\phi}_i \boldsymbol{\varphi}_i^T$, $\boldsymbol{\phi}_i$ ($i = 1, 2, \ldots, M_\theta$) and $\boldsymbol{\varphi}_j$ ($j = 1, 2, \ldots, M_\theta$) are first M_θ column vectors of matrices U and V, respectively. It is obvious that the minimum distance between the matrix A and B is $\sigma_{(M_\theta + 1)}$ and the matrix B is obtained with A_{M_θ} defined in Equation (36). A_{M_θ} is the optimal representation of A, and the optimal bases should be found in the structure of A_{M_θ}. Using the property of eigenvectors, it is well known that $\boldsymbol{\Phi} = (\boldsymbol{\phi}_1, \boldsymbol{\phi}_2, \ldots, \boldsymbol{\phi}_{M_\theta})$ ($M_\theta \leqslant L$) is a group of optimal bases that approximately represent the matrix A, and $\{\boldsymbol{\phi}_j\}_{j=1}^{M_\theta}$ are defined as the POD optimal bases.

Denote the L column vectors of the matrix A by $\boldsymbol{a}^l = (\theta_1^l, \theta_2^l, \ldots, \theta_m^l)^T$ ($l = 1, 2, \ldots, L$) and $\boldsymbol{\varepsilon}_l$ ($l = 1, 2, \ldots, L$) by unit column vectors except that a component is 1, whereas the other components are 0. Then by the compatibility of the norm for matrices and vectors, we have

$$\|\boldsymbol{a}^l - P_{M_\theta}(\boldsymbol{a}^l)\|_2 = \|(A - A_{M_\theta}) \boldsymbol{\varepsilon}_l\|_2 \leqslant \|A - A_{M_\theta}\|_{2,2} \|\boldsymbol{\varepsilon}_l\|_2$$
$$= \sigma_{M_\theta + 1} = \sqrt{\lambda_{M_\theta + 1}}, \quad l = 1, 2, \ldots, L \tag{37}$$

where $P_{M_\theta}(\boldsymbol{a}^l) = \sum\limits_{j=1}^{M_\theta} (\boldsymbol{\phi}_j, \boldsymbol{a}^l) \boldsymbol{\phi}_j$, $(\boldsymbol{\phi}_j, \boldsymbol{a}^l)$ is the canonical inner product for vector $\boldsymbol{\phi}_j$ and vector $\boldsymbol{a}^l$. Inequality (37) shows that $P_{M_\theta}(\boldsymbol{a}^l)$ is the optimal approximation to $\boldsymbol{a}^l$, and the error between them is less than or equal to $\sqrt{\lambda_{M_\theta + 1}}$.

3.2. Reduced implicit difference scheme based on proper orthogonal decomposition for two-dimensional unsaturated flow equation

The following work addresses how to use the POD bases found in order to restructure the reduced IDS for the two-dimensional unsaturated flow equation. Write

$$\boldsymbol{\theta}(t) = (\theta_1(t), \theta_2(t), \ldots, \theta_m(t))^T \tag{38}$$

where $\theta_i(t) = \theta_{j,k}(t)$ ($i = k(J + 1) + (j + 1), m = (J + 1)(K + 1), i = 1, 2, \ldots, m; j = 0, 1, 2, \ldots, J; k = 0, 1, 2, \ldots, K; t \in (0, T)$). Combine the equations (I), (II), (III), (IV), and (V), the discrete equations being rewritten as the following vector formulation:

$$A \boldsymbol{\theta}^{n+1} = \boldsymbol{\theta}^n + \frac{\Delta t}{\Delta z} F(\boldsymbol{\theta}^{n+1}), \ n = 0, 1, 2, \ldots, N - 1 \tag{39}$$

where A is a coefficient matrix about $\boldsymbol{\theta}^{n+1}$, $F(\boldsymbol{\theta}^{n+1})$ is the vector function obtained from the discrete equation. Put

$$\boldsymbol{\theta}^n = \boldsymbol{\Phi} \alpha_{M_\theta}^n \tag{40}$$

where $\boldsymbol{\theta}(t) = (\theta_1(t), \theta_2(t), \ldots, \theta_m(t))^T$, $\boldsymbol{\Phi} = (\boldsymbol{\phi}_1, \boldsymbol{\phi}_2, \ldots, \boldsymbol{\phi}_{M_\theta})$, and $\boldsymbol{\alpha}_{M_\theta} = (\alpha_1, \alpha_2, \ldots, \alpha_{M_\theta})^T$. Inserting Equation (40) into Equation (39) and noting that $\boldsymbol{\Phi}$ is the orthogonal matrix consisting of the POD bases, we can obtain the reduced IDS which has M_θ ($M_\theta \ll m$) unknown variables:

$$A\boldsymbol{\Phi}\boldsymbol{\alpha}_{M_\theta}^{n+1} = \boldsymbol{\Phi}\boldsymbol{\alpha}_{M_\theta}^n + \frac{\Delta t}{\Delta z}F\left(\boldsymbol{\Phi}\boldsymbol{\alpha}_{M_\theta}^{n+1}\right) \tag{41}$$

where $n = 0, 1, 2, \ldots, N$, and the initial values are $\boldsymbol{\alpha}_{M_\theta}^0 = \boldsymbol{\Phi}^T\boldsymbol{\theta}^0$.

Remark 2
Compared with Equation (39), it is obvious that Equation (41) has much fewer unknown variables. After one has obtained $\boldsymbol{\alpha}_{M_\theta}^n$ from Equation (41), one can obtain the POD optimal solutions, which are formulated as $\boldsymbol{\theta}^{*n} = \boldsymbol{\Phi}\boldsymbol{\alpha}_{M_\theta}^n$ by Equation (40), where $\boldsymbol{\theta}^{*n} = (\theta_1^{*n}, \theta_2^{*n}, \ldots, \theta_m^{*n})^T (i = k(J+1) + (j+1), m = (J+1)(K+1), i = 1, 2, \ldots, m; j = 0, 1, 2, \ldots, J; k = 0, 1, 2, \ldots, K; n = 0, 1, 2, \ldots, N-1)$. One only needs to solve Equation (41) with $M_\theta \times N$ ($M_\theta \ll L \ll m$) freedom degrees instead of the usual IDS (39) with $m \times N$ freedom degrees. Thus, both the computational load and memory requirements can be greatly reduced.

4. ERROR ANALYSIS

In this section, the error estimates between the true solution $\{\theta(i, t_n)\}_{i=1}^m$, usual IDS solution $\boldsymbol{\theta}^n$, and the reduced IDS solution $\boldsymbol{\theta}^{*n}$ based on POD bases are provided, and three theorems are obtained. We assume that the source term S_r is smooth enough. Because $0 < \underline{\theta} \leqslant \theta \leqslant \theta_s$, and $D(\theta)$ and $\tilde{K}(\theta)$ being sufficiently smooth, the solution θ for Equation (1) in Ω (where $\Omega = (0, M) \times (0, \tilde{M})$) belongs to Sobolev space $H^{r+2}(\Omega)$ ($r \geqslant 1$). However, because the computational domain is quadrilateral, $\theta \in H^2(\Omega_1)$ (where $\Omega_1 = ([0, M_1] \times [0, M_1]) \cup ([0, M_1] \times [\tilde{M} - M_1, \tilde{M}]) \cup ([M - M_1, M] \times [\tilde{M} - M_1, \tilde{M}]) \cup ([M - M_1, M] \times [0, M_1])$, $M_1 \geqslant 2 \max\{\triangle x, \triangle y\}$) in the vicinity of the corner point on $\partial\Omega$, according to the regularity of the nonlinear parabolic equation solutions [30]. Thus, the approximation error in the vicinity of the corner point (e.g., the subdomain $\Omega_1 \subset \Omega$) exists only in first-order accuracy, which is presented as the following result.

Theorem 1
The usual IDS solution $\theta_i^n \in \boldsymbol{\theta}^n$ for the two-dimensional unsaturated Equation (1) has the following error:

$$|E_n(\theta_i^n)| \equiv |\theta(i, t_n) - \theta_i^n| = O(\Delta t, \Delta x^2, \Delta z^2), \qquad \text{if } (x_j, z_k) \in \Omega/\Omega_1 \tag{42}$$

$$|E_n(\theta_i^n)| \equiv |\theta(i, t_n) - \theta_i^n| = O(\Delta t, \Delta x, \Delta z), \qquad \text{if } (x_j, z_k) \in \Omega_1 \tag{43}$$

where $m = (J+1)(K+1)$, $1 \leqslant i \leqslant m$, and $1 \leqslant n \leqslant N$ ($i = k(J+1) + (j+1)$; $j = 0, 1, 2, \ldots, J; k = 0, 1, 2, \ldots, K$).

Proof
First, if $(x_j, z_k) \in \Omega/\Omega_1$, $\theta_{j,k} \in H^{r+2}(\Omega/\Omega_1)$ ($r \geqslant 1$) as we discuss in preceding text. Expanding each term of Equation (31) at node (x_j, z_k) in a Taylor expansion, we have

$$\theta_{j,k}^n = \theta_{j,k}^{n+1} + (-\Delta t)\left(\frac{\partial\theta}{\partial t}\right)_{j,k}^{n+1} + \frac{(-\Delta t)^2}{2!}\left(\frac{\partial^2\theta}{\partial t^2}\right)_{j,k}^{n+1} + \frac{(-\Delta t)^3}{3!}\left(\frac{\partial^3\theta}{\partial t^3}\right)_{j,k}^{n+1} + \cdots \tag{44}$$

$$D_{j+\frac{1}{2},k}^{n+1} = D_{j,k}^{n+1} + \left(\frac{\Delta x}{2}\right)\left(\frac{\partial D}{\partial x}\right)_{j,k}^{n+1} + \frac{1}{2!}\left(\frac{\Delta x}{2}\right)^2\left(\frac{\partial^2 D}{\partial x^2}\right)_{j,k}^{n+1} + \frac{1}{3!}\left(\frac{\Delta x}{2}\right)^3\left(\frac{\partial^3 D}{\partial x^3}\right)_{j,k}^{n+1} + \cdots \tag{45}$$

$$\theta_{j+1,k}^{n+1} = \theta_{j,k}^{n+1} + (\Delta x)\left(\frac{\partial\theta}{\partial x}\right)_{j,k}^{n+1} + \frac{1}{2!}(\Delta x)^2\left(\frac{\partial^2\theta}{\partial x^2}\right)_{j,k}^{n+1} + \frac{1}{3!}(\Delta x)^3\left(\frac{\partial^3\theta}{\partial x^3}\right)_{j,k}^{n+1} + \cdots \quad (46)$$

$$D_{j-\frac{1}{2},k}^{n+1} = D_{j,k}^{n+1} - \left(\frac{\Delta x}{2}\right)\left(\frac{\partial D}{\partial x}\right)_{j,k}^{n+1} + \frac{1}{2!}\left(-\frac{\Delta x}{2}\right)^2\left(\frac{\partial^2 D}{\partial x^2}\right)_{j,k}^{n+1} - \frac{1}{3!}\left(\frac{\Delta x}{2}\right)^3\left(\frac{\partial^3 D}{\partial x^3}\right)_{j,k}^{n+1} + \cdots$$
$$(47)$$

$$\theta_{j-1,k}^{n+1} = \theta_{j,k}^{n+1} + (-\Delta x)\left(\frac{\partial\theta}{\partial x}\right)_{j,k}^{n+1} + \frac{1}{2!}(-\Delta x)^2\left(\frac{\partial^2\theta}{\partial x^2}\right)_{j,k}^{n+1} + \frac{1}{3!}(-\Delta x)^3\left(\frac{\partial^3\theta}{\partial x^3}\right)_{j,k}^{n+1} + \cdots$$
$$(48)$$

$$D_{j,k+\frac{1}{2}}^{n+1} = D_{j,k}^{n+1} + \left(\frac{\Delta z}{2}\right)\left(\frac{\partial D}{\partial z}\right)_{j,k}^{n+1} + \frac{1}{2!}\left(\frac{\Delta z}{2}\right)^2\left(\frac{\partial^2 D}{\partial z^2}\right)_{j,k}^{n+1} + \frac{1}{3!}\left(\frac{\Delta z}{2}\right)^3\left(\frac{\partial^3 D}{\partial z^3}\right)_{j,k}^{n+1} + \cdots$$
$$(49)$$

$$\theta_{j,k+1}^{n+1} = \theta_{j,k}^{n+1} + (\Delta z)\left(\frac{\partial\theta}{\partial z}\right)_{j,k}^{n+1} + \frac{1}{2!}(\Delta z)^2\left(\frac{\partial^2\theta}{\partial z^2}\right)_{j,k}^{n+1} + \frac{1}{3!}(\Delta z)^3\left(\frac{\partial^3\theta}{\partial z^3}\right)_{j,k}^{n+1} + \cdots \quad (50)$$

$$D_{j,k-\frac{1}{2}}^{n+1} = D_{j,k}^{n+1} - \left(\frac{\Delta z}{2}\right)\left(\frac{\partial D}{\partial z}\right)_{j,k}^{n+1} + \frac{1}{2!}\left(-\frac{\Delta z}{2}\right)^2\left(\frac{\partial^2 D}{\partial z^2}\right)_{j,k}^{n+1} - \frac{1}{3!}\left(\frac{\Delta z}{2}\right)^3\left(\frac{\partial^3 D}{\partial z^3}\right)_{j,k}^{n+1} + \cdots$$
$$(51)$$

$$\theta_{j,k-1}^{n+1} = \theta_{j,k}^{n+1} + (-\Delta z)\left(\frac{\partial\theta}{\partial z}\right)_{j,k}^{n+1} + \frac{1}{2!}(-\Delta z)^2\left(\frac{\partial^2\theta}{\partial z^2}\right)_{j,k}^{n+1} + \frac{1}{3!}(-\Delta z)^3\left(\frac{\partial^3\theta}{\partial z^3}\right)_{j,k}^{n+1} + \cdots$$
$$(52)$$

$$\tilde{K}_{j,k+\frac{1}{2}}^{n+1} = \tilde{K}_{j,k}^{n+1} + \left(\frac{\Delta z}{2}\right)\left(\frac{\partial\tilde{K}}{\partial z}\right)_{j,k}^{n+1} + \frac{1}{2!}\left(\frac{\Delta z}{2}\right)^2\left(\frac{\partial^2\tilde{K}}{\partial z^2}\right)_{j,k}^{n+1} + \frac{1}{3!}\left(\frac{\Delta z}{2}\right)^3\left(\frac{\partial^3\tilde{K}}{\partial z^3}\right)_{j,k}^{n+1} + \cdots$$
$$(53)$$

$$\tilde{K}_{j,k-\frac{1}{2}}^{n+1} = \tilde{K}_{j,k}^{n+1} - \left(\frac{\Delta z}{2}\right)\left(\frac{\partial\tilde{K}}{\partial z}\right)_{j,k}^{n+1} + \frac{1}{2!}\left(-\frac{\Delta z}{2}\right)^2\left(\frac{\partial^2\tilde{K}}{\partial z^2}\right)_{j,k}^{n+1} - \frac{1}{3!}\left(\frac{\Delta z}{2}\right)^3\left(\frac{\partial^3\tilde{K}}{\partial z^3}\right)_{j,k}^{n+1} + \cdots$$
$$(54)$$

Inserting Equations (44)–(54) into Equation (31), we have

$$\left(\frac{\partial\theta}{\partial t} - \frac{\partial}{\partial x}\left(D(\theta)\frac{\partial\theta}{\partial x}\right) - \frac{\partial}{\partial z}\left(D(\theta)\frac{\partial\theta}{\partial z}\right) + \frac{\partial\tilde{K}(\theta)}{\partial z}\right)_{j,k}^{n+1} = \frac{\Delta t}{2}\left(\frac{\partial^2\theta}{\partial t^2}\right)_{j,k}^{n+1}$$
$$+ \frac{1}{24}(\Delta x)^2\left(\frac{\partial\theta}{\partial x}\frac{\partial^3 D}{\partial x^3}\right)_{j,k}^{n+1} + \frac{1}{8}(\Delta x)^2\left(\frac{\partial^2\theta}{\partial x^2}\frac{\partial^2 D}{\partial x^2}\right)_{j,k}^{n+1} + \frac{1}{6}(\Delta x)^2\left(\frac{\partial^3\theta}{\partial x^3}\frac{\partial D}{\partial x}\right)_{j,k}^{n+1} +$$
$$\frac{1}{24}(\Delta z)^2\left(\frac{\partial\theta}{\partial z}\frac{\partial^3 D}{\partial z^3}\right)_{j,k}^{n+1} + \frac{1}{8}(\Delta z)^2\left(\frac{\partial^2\theta}{\partial z^2}\frac{\partial^2 D}{\partial z^2}\right)_{j,k}^{n+1} + \frac{1}{6}(\Delta z)^2\left(\frac{\partial^3\theta}{\partial z^3}\frac{\partial D}{\partial z}\right)_{j,k}^{n+1} + \cdots \quad (55)$$

Note that $\theta_i = \theta_{j,k}(i = k(J+1) + (j+1), m = (J+1)(K+1), i = 1, 2, \ldots, m; j = 0, 1, 2, \ldots, J; k = 0, 1, 2, \ldots, K)$. Thus, when the usual IDS (32) approaches the PDE (1), the truncation error (TE) is given by

$$\text{TE} = O\left(\Delta t, \Delta x^2, \Delta z^2\right) \tag{56}$$

Second, if $(x_j, z_k) \in \Omega_1$, then $\theta_{j,k} \in H^2(\Omega_1)$ as we discuss in preceding text. According to the definition of Sobolev space $H^2(\Omega_1)$, Equations (46), (48), (50), and (52) can be written as follows:

$$\theta_{j+1,k}^{n+1} = \theta_{j,k}^{n+1} + (\Delta x)\left(\frac{\partial \theta}{\partial x}\right)_{j,k}^{n+1} + \frac{1}{2!}(\Delta x)^2\left(\frac{\partial^2 \theta(\xi_1, z_k, t_{n+1})}{\partial x^2}\right), \quad \xi_1 \in (x_j, x_j + \Delta x) \tag{57}$$

$$\theta_{j-1,k}^{n+1} = \theta_{j,k}^{n+1} + (-\Delta x)\left(\frac{\partial \theta}{\partial x}\right)_{j,k}^{n+1} + \frac{1}{2!}(-\Delta x)^2\left(\frac{\partial^2 \theta(\xi_2, z_k, t_{n+1})}{\partial x^2}\right), \quad \xi_2 \in (x_j - \Delta x, x_j) \tag{58}$$

$$\theta_{j,k+1}^{n+1} = \theta_{j,k}^{n+1} + (\Delta z)\left(\frac{\partial \theta}{\partial z}\right)_{j,k}^{n+1} + \frac{1}{2!}(\Delta z)^2\left(\frac{\partial^2 \theta(x_j, \eta_1, t_{n+1})}{\partial z^2}\right), \quad \eta_1 \in (z_k, z_k + \Delta z) \tag{59}$$

$$\theta_{j,k-1}^{n+1} = \theta_{j,k}^{n+1} + (-\Delta z)\left(\frac{\partial \theta}{\partial z}\right)_{j,k}^{n+1} + \frac{1}{2!}(-\Delta z)^2\left(\frac{\partial^2 \theta(x_j, \eta_2, t_{n+1})}{\partial z^2}\right), \quad \eta_2 \in (z_k - \Delta z, z_k) \tag{60}$$

Combining Equations (44) and (1), we have

$$\text{TE} = O\left(\Delta t, \Delta x, \Delta z\right) \tag{61}$$

$\square$

Theorem 2
Let $\boldsymbol{\theta}^n$ $(n = 1, 2, \ldots, N)$ be vectors constituted with solutions of usual IDS (39) and $\boldsymbol{\theta}^{*n}$ $(n = 1, 2, \ldots, N)$ the vectors constituted with solutions of the reduced optimizing IDS (41). If $n \in \{1, 2, \ldots, L\}$, the error estimates are obtained as follows:

$$\|\boldsymbol{\theta}_m^n - \boldsymbol{\theta}^{*n}\|_2 \leqslant \sqrt{\lambda_{M_\theta+1}}, \qquad n \in \{1, 2, \ldots, L\} \tag{62}$$

Else if $n \notin \{1, 2, \ldots, L\}$, when t_l $(1 \leqslant l \leqslant L)$ are uniformly chosen from t_n $(1 \leqslant n \leqslant N)$, and $\left\|\frac{\partial \theta(\xi_1)}{\partial t}\right\|_2$ and $\left\|\frac{\partial \theta^*(\xi_2)}{\partial t}\right\|_2$ are bounded (i.e., $\left\|\frac{\partial \theta(\xi_1)}{\partial t}\right\|_2 \leqslant C$ and $\left\|\frac{\partial \theta^*(\xi_2)}{\partial t}\right\|_2 \leqslant C$), the following error estimates exist:

$$\|\boldsymbol{\theta}^n - \boldsymbol{\theta}^{*n}\|_2 \leqslant \sqrt{\lambda_{M_\theta+1}} + \frac{\Delta t N}{2L}C, \qquad n \notin \{1, 2, \ldots, L\} \tag{63}$$

where $\|\bullet\|$ is a vector norm, $1 \leqslant i \leqslant m$ and $m = (J+1)(K+1)$.

Proof
Let

$$\chi = \text{span}\{\boldsymbol{\phi}_1, \boldsymbol{\phi}_2, \ldots, \boldsymbol{\phi}_{M_\theta}\} \tag{64}$$

Then, for column vectors $\boldsymbol{a}^l$ $(1 \leqslant l \leqslant L)$ of the matrix $\boldsymbol{A}$, by Equation (37), we have $\boldsymbol{a}^l = \boldsymbol{\theta}^l$, and there is a $P_{M_\theta}\left(\boldsymbol{\theta}^l\right) = P_{M_\theta}\left(\boldsymbol{a}^l\right) = \sum_{j=1}^{M_\theta}\left(\boldsymbol{\phi}_j, \boldsymbol{a}^l\right)\boldsymbol{\phi}_j = \sum_{j=1}^{M_\theta}\left(\boldsymbol{\phi}_j, \boldsymbol{\theta}^l\right)\boldsymbol{\phi}_j \in \chi$ such that

$$\|\boldsymbol{\theta}^l - P_{M_\theta}\left(\boldsymbol{\theta}^l\right)\|_2 \leqslant \sqrt{\lambda_{M_\theta+1}}, \qquad 1 \leqslant l \leqslant L \tag{65}$$

If $n = l \in \{1, 2, \ldots, L\}$, $\boldsymbol{\theta}^{*n} = P_{M_\theta}(\boldsymbol{\theta}^n) = \sum_{j=1}^{M_\theta} (\boldsymbol{\phi}_j, \boldsymbol{\theta}^n) \boldsymbol{\phi}_j$ is obtained by the formula (40) and (41); therefore, we have

$$\|\boldsymbol{\theta}^n - \boldsymbol{\theta}^{*n}\|_2 \leqslant \sqrt{\lambda_{M_\theta+1}}, \quad n \in \{1, 2, \ldots, L\} \tag{66}$$

If $n \notin \{1, 2, \ldots, L\}$, we assume that $t_n \in (t_{l-1}, t_l)$, and t_n is the nearest point to t_l. $\boldsymbol{\theta}^n$ and $\boldsymbol{\theta}^{*n}$ are expanded in a Taylor series expansion at point t_l, respectively.

$$\boldsymbol{\theta}^n = \boldsymbol{\theta}^l - s\Delta t \frac{\partial \boldsymbol{\theta}(\zeta_1)}{\partial t}, \quad t_n \leqslant \zeta_1 \leqslant t_l \tag{67}$$

$$\boldsymbol{\theta}^{*n} = \boldsymbol{\theta}^{*l} - s\Delta t \frac{\partial \boldsymbol{\theta}^*(\zeta_2)}{\partial t}, \quad t_n \leqslant \zeta_2 \leqslant t_l \tag{68}$$

where s is the number of time steps from t_n to t_l. If t_l $(1 \leqslant l \leqslant L)$ are uniformly chosen from t_n $(1 \leqslant n \leqslant N)$, we have $s \leqslant \frac{N}{2L}$. Moreover, when $\left\|\frac{\partial \boldsymbol{\theta}(\zeta_1)}{\partial t}\right\|_2$ and $\left\|\frac{\partial \boldsymbol{\theta}^*(\zeta_2)}{\partial t}\right\|_2$ are bounded (i.e., $\left\|\frac{\partial \boldsymbol{\theta}(\zeta_1)}{\partial t}\right\|_2 \leqslant C$ and $\left\|\frac{\partial \boldsymbol{\theta}^*(\zeta_2)}{\partial t}\right\|_2 \leqslant C$), by subtracting Equation (68) from Equation (67), we can obtain that

$$
\begin{aligned}
\|\boldsymbol{\theta}^n - \boldsymbol{\theta}^{*n}\|_2 &= \left\|\boldsymbol{\theta}^l - \boldsymbol{\theta}^{*l} - s\Delta t \left(\frac{\partial \boldsymbol{\theta}(\zeta_1)}{\partial t} - \frac{\partial \boldsymbol{\theta}^*(\zeta_2)}{\partial t}\right)\right\|_2 \\
&\leqslant \|\boldsymbol{\theta}^l - \boldsymbol{\theta}^{*l}\|_2 + s\Delta t \left\|\frac{\partial \boldsymbol{\theta}(\zeta_1)}{\partial t} - \frac{\partial \boldsymbol{\theta}^*(\zeta_2)}{\partial t}\right\|_2 \\
&\leqslant \|\boldsymbol{\theta}^l - \boldsymbol{\theta}^{*l}\|_2 + s\Delta t \left[\left\|\frac{\partial \boldsymbol{\theta}(\zeta_1)}{\partial t}\right\|_2 + \left\|\frac{\partial \boldsymbol{\theta}^*(\zeta_2)}{\partial t}\right\|_2\right] \\
&\leqslant \sqrt{\lambda_{M_\theta+1}} + \frac{\Delta t N}{2L} C, \quad n \notin \{1, 2, \ldots, L\}
\end{aligned}
$$

$\square$

Theorem 3
Under the assumptions of Theorem 2, let $\sqrt{\lambda_{M_\theta+1}} = O(\Delta t)$; the following error estimate holds

$$|\theta(j, k, t_n) - \theta_{j,k}^{*n}| = O\left(\Delta t + \sqrt{\lambda_{M_\theta+1}}, \Delta x^2, \Delta z^2\right), 1 \leqslant n \leqslant N, \quad \text{if } (x_j, z_k) \in \Omega/\Omega_1 \tag{69}$$

$$|\theta(j, k, t_n) - \theta_{j,k}^{*n}| = O\left(\Delta t + \sqrt{\lambda_{M_\theta+1}}, \Delta x, \Delta z\right), 1 \leqslant n \leqslant N, \quad \text{if } (x_j, z_k) \in \Omega_1 \tag{70}$$

where $1 \leqslant j \leqslant J$ and $1 \leqslant k \leqslant K$.

Proof
Note that the absolute value of each component of a vector is not more than any norm of the vector. Combining Theorems 1 and 2, we have

$$
\begin{aligned}
|\theta(i, t_n) - \theta_i^{*n}| &= |\theta(i, t_n) - \theta_i^n + \theta_i^n - \theta_i^{*n}| \leqslant |\theta(i, t_n) - \theta_i^n| + |\theta_i^n - \theta_i^{*n}| \\
&= O\left(\Delta t + \sqrt{\lambda_{M_\theta+1}}, \Delta x^2, \Delta z^2\right), \qquad 1 \leqslant n \leqslant N, \quad \text{if } (x_j, z_k) \in \Omega/\Omega_1
\end{aligned}
$$

$$
\begin{aligned}
|\theta(i, t_n) - \theta_i^{*n}| &= |\theta(i, t_n) - \theta_i^n + \theta_i^n - \theta_i^{*n}| \leqslant |\theta(i, t_n) - \theta_i^n| + |\theta_i^n - \theta_i^{*n}| \\
&= O\left(\Delta t + \sqrt{\lambda_{M_\theta+1}}, \Delta x, \Delta z\right), \qquad 1 \leqslant n \leqslant N, \quad \text{if } (x_j, z_k) \in \Omega_1
\end{aligned}
$$

$\square$

5. NUMERICAL EXPERIMENT

In this section, a numerical example of the two-dimensional unsaturated soil flow model is conducted to validate the feasibility and efficiency of the POD method. The computational domain consists of a square vertical profile with dimensions 50 cm × 50 cm. θ_0 and θ_s are 0.16 and 0.48, respectively. Let $M_1 = \tilde{M}_1 = 1$ cm such that the initial value is continuous. The source term S_r is taken as 0. As the singular boundary source $\theta(0, 0, t) = \theta_s$ is used, the single moderate grid is not suitable for the numerical test. In accordance with Theorem 1, the uniform horizontal (vertical) space step is 0.1 cm for the whole domain $[0, M] \times [0, \tilde{M}]$, and the uniform horizontal (vertical) space step is 0.01 cm for the subdomain $[0, M_1] \times [0, \tilde{M}_1]$. The uniform time step Δt is 0.02 h. We obtain 20 discrete values (i.e., snapshots) at time $t = 1$ h, 2 h, 3 h, ..., 20 h by solving the usual IDS (39).

When $t = 20$ h, we obtain the solutions of the reduced IDS (40) and (41) depicted on the right-hand sides of Figure 3, where the number of POD bases M_θ is 7, whereas the solutions of usual IDS (39) are depicted on the left-hand side of Figures 3 (because this figure is almost equal to the solutions obtained with 20 POD bases, it is also referred to as the figure with full bases). Figure 4 is the result of rotating Figure 3 by 180°.

In order to further compare the difference between the usual IDS solutions and the reduced IDS solutions, the contour isolines of soil moisture content and the figure of wetting front (i.e., $\theta = 0.2$) are illustrated. Figure 5 shows the contour isolines plot of soil moisture content when $t = 20$ h. The usual IDS solutions are depicted on the left-hand side, whereas the reduced IDS solutions with seven POD bases are depicted on the right-hand side. The wetting front (i.e., $\theta = 0.2$) is drawn once every 4 h for 20 h, the results of which are shown in Figure 6.

The phenomenon that the vertical movement is faster than the horizontal movement is illustrated in Figure 6. Likewise, the usual IDS solutions and the reduced IDS solutions are depicted on the left-hand side and right-hand side, respectively. Figure 7 shows the mean absolute error (MAE) between solutions obtained with different number of POD bases and the solutions obtained with full bases. By implementing the numerical simulation of the soil moisture content for 20 h, we find that the central processing unit (CPU) time consumed by the usual IDS is 112 s, whereas that of the reduced IDS with seven POD bases is only 1 s (i.e., the CPU time required by the usual IDS is 111 times larger than that of the reduced IDS with seven POD bases), and the MAE between the solutions does not exceed 4.6×10^{-3}, which is the result of numerical computing, whereas $\sqrt{\lambda_8} = 0.03$ and the error 0.052 obtained by Equation (63). Moreover, we find that the MAEs on $[0, 1] \times [0, 1]$ are approximately those on $\Omega \backslash ([0, 1] \times [0, 1])$, which shows that the results obtained for the numerical example are consistent with those obtained for the theoretical ones, but the numerical results are
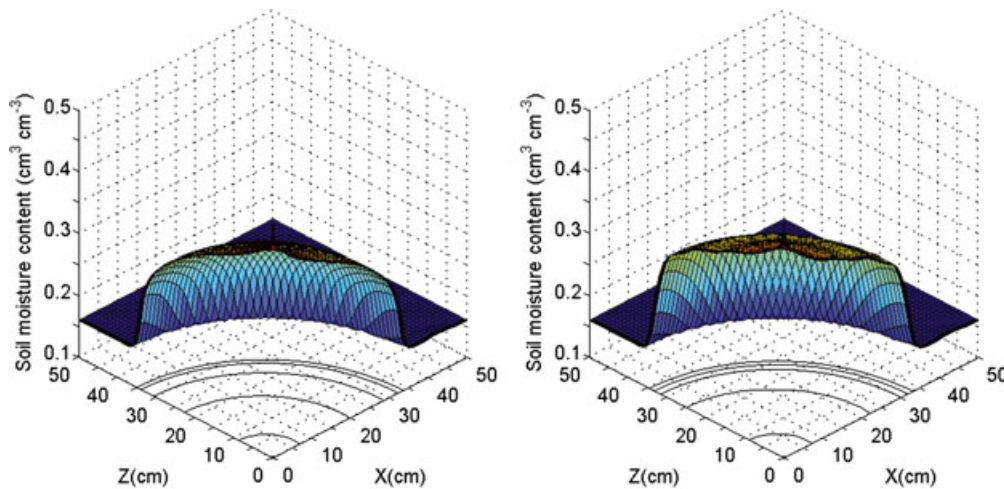
Figure 3. When $t = 20$ h, the soil moisture figure for full bases solutions (left-hand side figure) and $M_\theta = 7$ solutions of reduced IDS based on POD (right-hand side figure).
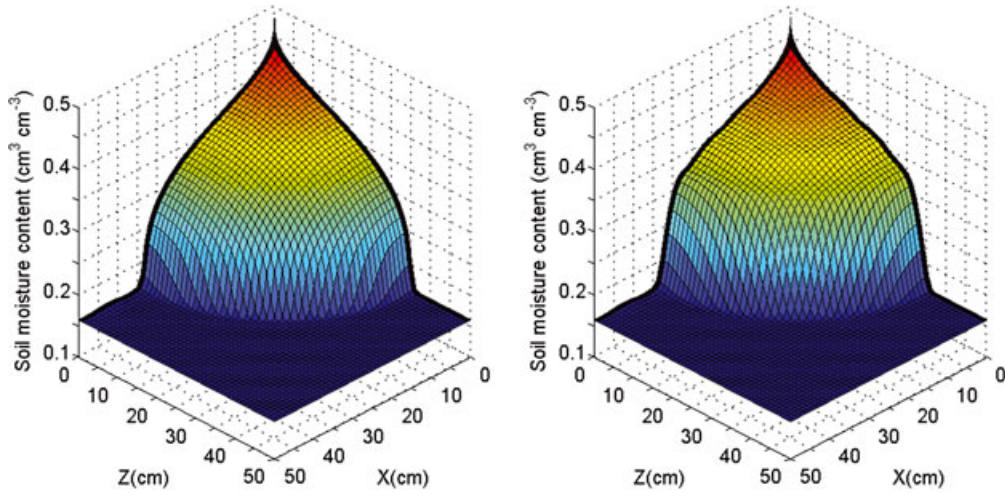
Figure 4. The results of rotating Figure 3 by 180°.
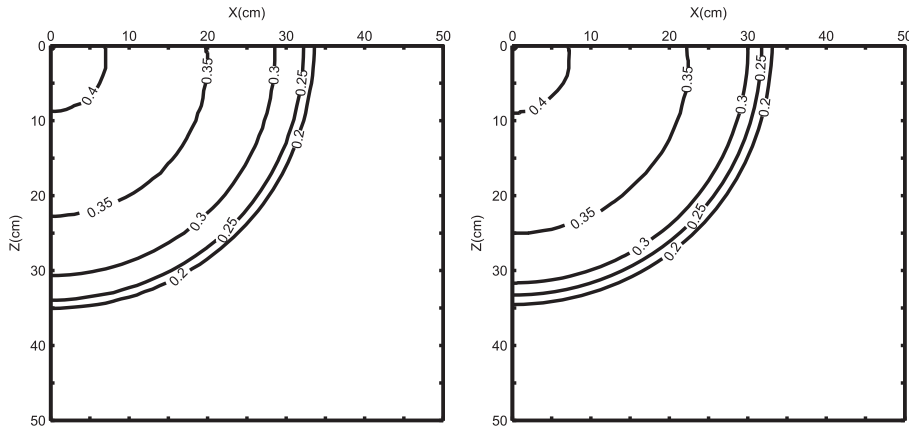
Figure 5. When $t = 20$ h, the contour isolines plot of soil moisture content for full bases solutions (left-hand side figure) and $M_\theta = 7$ solutions of reduced IDS based on POD (right-hand side figure).
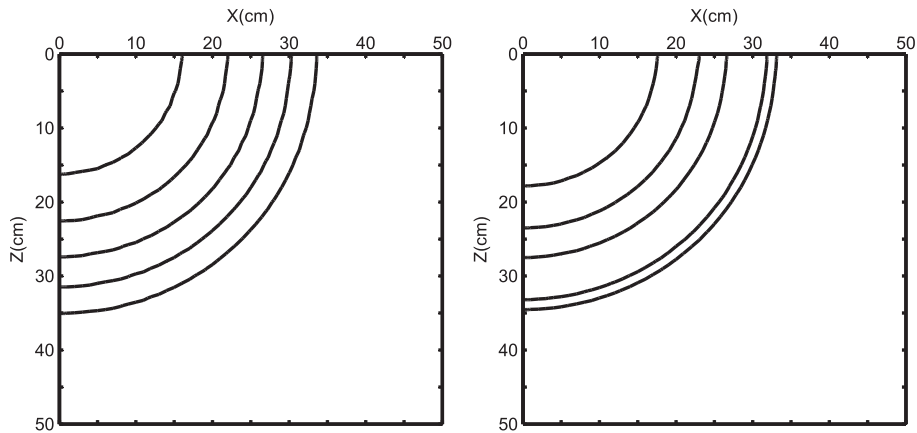
Figure 6. The variation of wetting front (i.e., $\theta = 0.2$) in 20 h for full bases solutions (left-hand side figure) and $M_\theta = 7$ solutions of reduced IDS based on POD (right-hand side figure). In each subplot, the result is plotted once every 4 h.
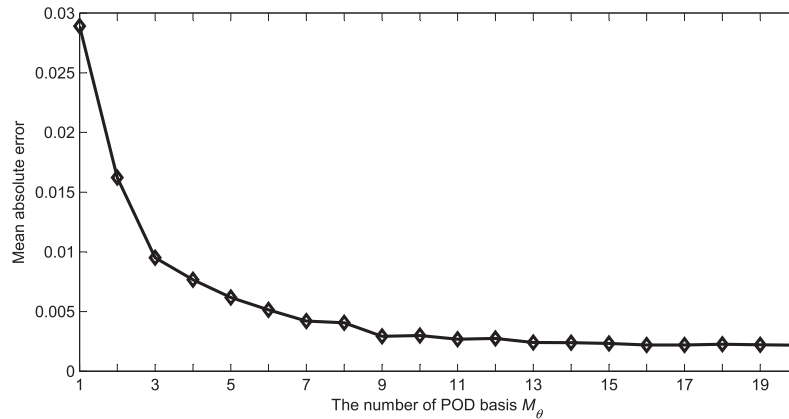
Figure 7. The mean absolute error for different number of POD bases.

better than the theoretical results (also see Figure 7). Also, the memory requirements in the computational process are greatly reduced. It is also found that the POD method is very effective in solving the two-dimensional equation with high number of degrees of freedom. Although what we have done here is a re-computation in order to validate the POD method, when it comes to actual problems, we may structure the snapshots and POD bases with interpolation or data assimilation for samples from experiments and then solve directly the optimizing reduced IDS. Moreover, because the two-dimensional unsaturated flow equation includes θ_s (usually the empirical saturate value of soil moisture), θ_0 (usually taken as the residual value of soil moisture), and other parameters, POD basis is dependent on these given data, which vary with them.

6. CONCLUSIONS

In this paper, an optimizing reduced IDS for the two-dimensional unsaturated flow equation is presented by implementing the SVD and POD techniques into the usual IDS of the corresponding equation. The ensemble of data is compiled from transient solutions obtained with the usual IDS. However, in actual applications, the ensemble of snapshots is usually obtained from the physical system trajectories by drawing samples from experiments and interpolation (or data assimilation). We then implemented the SVD technique for deriving POD basis from the ensemble of data and substituted the usual IDS with the optimizing reduced IDS, based on the POD basis. Because only few bases in the POD basis are used, the reduced IDS is optimal. We have analyzed the error between the POD reduced IDS solution and the usual IDS solution. It is shown by using a numerical example that the error between the POD approximate solution and the full IDS solution is consistent with the theoretical error results derived. Thus, both the feasibility and efficiency of our reduced IDS are validated. The theoretical and numerical results in this paper also demonstrate that the method has extensive potential applications in solving complicated systems of nonlinear PDEs by using the POD method to structure the optimizing reduced IDS from the usual IDS.

REFERENCES

1. Xie ZH, Zeng QC, Dai YJ, Wang B. Numerical simulation of an unsaturated flow equation. *Science in China Series D: Earth Sciences* 1998; **41**:429–436.
2. Luo ZD, Xie ZH, Zhu J, Zeng QC. Mixed finite element method and numerical simulation for the unsaturated soil water flow problem. *Mathematica Numerica, Sinica* 2003; **25**:113–128. (in Chinese).

3. Lei ZD, Yang SX, Xie SC. *Soil Water Dynamics*. Tsinghua University Press: Beijing, 1988. (in Chinese).
4. Fukunaga K. *Introduction to Statistical Recognition*. Academic Press: New York, 1990.
5. Jolliffe IT. *Principal Component Analysis*. Springer: New York, 2002.
6. Holmes P, Lumley J, Berkooz G. *Turbulence, Coherent Structures, Dynamical Systems and Symmetry*. Cambridge University Press: Cambridge, 1996.
7. Moin P, Moser R. Characteristic-eddy decomposition of turbulence in channel. *Journal of Fluid Mechanics* 1989; **200**:471–509.
8. Rajaee M, Karlsson S, Sirovich L. Low dimensional description of free shear flow coherent structures and their dynamical behavior. *Journal of Fluid Mechanics* 1994; **258**:1–29.
9. Joslin R, Gunzburger M, Nicolaides R, Erlebacher G, Hussaini M. A self-contained automated methodology for optimal flow control validated for transition delay. *AIAA Journal* 1997; **35**:816–824.
10. Ly H, Tran H. Proper orthogonal decomposition for flow calculations and optimal control in a horizontal CVD reactor. *Quarterly of Applied Mathematics* 2002; **60**:631–656.
11. Lumley J. Coherent structures in turbulence. In *Transition and Turbulence*, Meyer RE (ed.). Academic Press: New York, 1981.
12. Aubry N, Holmes P, Lumley J, Stone E. The dynamics of coherent structures in the wall region of a turbulent boundary layer. *Journal of Fluid Dynamics* 1998; **192**:115–173.
13. Sirovich L. Turbulence and the dynamics of coherent structures: Part I–III. *Quarterly of Applied Mathematics* 1987; **45**:561–590.
14. Kunisch K, Volkwein S. Galerkin proper orthogonal decomposition methods for parabolic problems. *Numerische Mathematik* 2001; **90**:117–148.
15. Kunisch K, Volkwein S. Galerkin proper orthogonal decomposition methods for a general equation in fluid dynamics. *SIAM Journal on Numerical Analysis* 2002; **40**:492–515.
16. Luo ZD, Wang RW, Zhu J. Finite difference scheme based on proper orthogonal decomposition for the non-stationary Navier–Stokes equations. *Science in China Series A: Mathematics* 2007; **50**:1186–1196.
17. Luo ZD, Chen J, Navon IM, Yang XZ. Mixed finite element formulation and error estimates based on proper orthogonal decomposition for the non-stationary Navier–Stokes equations. *SIAM Journal on Numerical Analysis* 2008; **47**:1–19.
18. Luo ZD, Chen J, Sun P, Yang XZ. Finite element formulation based on proper orthogonal decomposition for parabolic equations. *Science in China Series A: Mathematics* 2009; **52**:587–596.
19. Luo ZD, Yang XZ, Zhou YJ. A reduced finite element formulation based on proper orthogonal decomposition for Burgers equation. *Applied Numerical Mathematics* 2009; **59**:1933–1946.
20. Cao YH, Zhu J, Luo ZD, Navon IM. Reduced order modeling of the upper tropical Pacific ocean model using proper orthogonal decomposition. *Computers & Mathematics with Applications* 2006; **52**:1373–1386.
21. Cao YH, Zhu J, Navon IM, Luo ZD. A reduced order approach to four-dimensional variational data assimilation using proper orthogonal decomposition. *International Journal for Numerical Methods in Fluids* 2007; **53**:1571–1583.
22. Luo ZD, Zhu J, Wang RW, Navon IM. Proper orthogonal decomposition approach and error estimation of mixed finite element methods for the tropical Pacific Ocean reduced gravity model. *Computer Methods in Applied Mechanics and Engineering* 2007; **196**:4184–4195.
23. Luo ZD, Chen J, Zhu J, Wang RW, Navon IM. An optimizing reduced order FDS for the tropical Pacific Ocean reduced gravity model. *International Journal for Numerical Methods in Fluids* 2007; **55**:143–161.
24. Wang RW, Zhu J, Luo ZD, Navon IM. An equation-free reduced order modeling approach to tropic Pacific simulation. *Advances in Geosciences* 2007; **12**:1–16.
25. Du J, Zhu J, Luo ZD, Navon IM. An optimizing finite difference scheme based on proper orthogonal decomposition for CVD equations. *International Journal for Numerical Methods in Biomedical Engineering* 2011; **27**:78–94.
26. Yu HL, Chu HJ. Understanding space–time patterns of groundwater system by empirical orthogonal functions: a case study in the Choshui River alluvial fan, Taiwan. *Journal of Hydrology* 2010; **381**:239–247.
27. Bernard T, Krol O, Linke H, Rauschenbach T. Optimal management of regional water supply systems using a reduced finite-element groundwater model. *Automatisierungstechnik* 2008; **57**:593–600.
28. Bear J. *Dynamics of Fluids in Porous Media*. American Elsevier Publishing Company: New York, 1972.
29. Clapp R, Hornberger G. Empirical equation for some soil hydraulic properties. *Water Resource Research* 1978; **14**:601–604.
30. Chen YZ. *Second Order Parabolic Partial Differential Equations*. Peking University Press: Beijing, 2003.